Effect of copper on structural, optical and electrochemical properties of SnO$_2$ nanoparticles

M. PARTHIBAVARMAN[a], V. HARIHARAN[a], C. SEKAR[a,b*], V. N. SINGH[c]

[a]Centre for Nanoscience and Technology, Department of Physics, Periyar University, Salem - 636011, India
[b]Department of Bioelectronics and Biosensors, Alagappa University, Karaikudi - 630003
[c]Thin Film Laboratory, Department of Physics, Indian Institute of Technology, Hauz Khas, New Delhi-110016, India

Pure and Cu doped SnO$_2$ nanopowders have been synthesized by chemical precipitation method using SnCl$_4$.5H$_2$O, NH$_3$.H$_2$O and CuSO$_4$.5H$_2$O as raw materials. The products have been annealed at 600°C for 5 hours under ambient condition in order to improve the crystallinity. Powder XRD results show that the samples crystallize in tetragonal rutile type SnO$_2$ phase. The average crystalline size of pure SnO$_2$ is found to be around 10 nm. The crystal structure of the SnO$_2$ does not change with the introduction of Cu, but the crystalline size decreases to 8 nm and 6.5 nm for Cu doping of 10 & 20 wt.% respectively. These results have been confirmed by the transmission electron microscopy (TEM) studies. UV-VIS diffusion reflectance spectroscopy (DRS) revealed the band gap energies to be 3.56, 3.31, 3.28 eV for pure and Cu (10 & 20 wt.%) doped SnO$_2$ respectively. Temperature dependent resistivity measurement showed that both the pure and Cu doped samples are suitable for gas sensing applications. The electrochemical nature of the samples has been studied using cyclic voltammetric method.

1. Introduction

Transition – metal oxide nanomaterials, such as SnO$_2$, ZnO, TiO$_2$ and WO$_3$ have attracted extensive research interests owing to their unique physical and chemical properties and diverse potential applications in optical and electronic fields. SnO$_2$ is a wide band gap (E$_g$ = 3.6 eV) semiconductor with n-type conduction due to the existence of intrinsic defects and has been widely used in many fields, such as photocatalysis, transparent conducting electrodes for flat panel displays and solar cells, gas sensors and oxidation catalyst, owing to its outstanding optical and electrical properties accompanied with super mechanical and chemical stability [1]. Many processes have been developed for the synthesis of SnO$_2$ nanostructures, e.g. spray pyrolysis [2], hydrothermal methods [3], evaporating tin grains in air [4], chemical vapor deposition (CVD) [5], thermal evaporation of oxide powders [6], rapid oxidation of elemental tin [7] and sol–gel method [8]. Doping with CuO has been shown to enhance the sensitivity and selectivity of SnO$_2$ toward H$_2$S. In comparison to pure SnO$_2$, SnO$_2$: CuO films show a high resistivity in air which drastically drops in presence of H$_2$S or other sulfur compounds. This behavior has been attributed to the formation of p–n heterojunctions (p-CuO and n-SnO$_2$), which induces an electron depleted space charge layer at the surface of SnO$_2$. Upon exposure to H$_2$S, the p-type semi-conducting CuO particles are converted to

CuS having metallic properties [9]. SnO$_2$ nanoparticles have been successfully doped with rare earth ion (Tb^{3+}, Eu3$^+$, and Ce^{3+}) and transition metal ion (Mn^{2+}) [10]. Many results have shown that the several additives (metal cations: Al, Co, Fe, Cu) can lead to an increase in the surface area of SnO$_2$ based powders [11]. Lee et al. reported that the added active element (Eu) stabilize the SnO$_2$ surface and promote decrease in grain size [12]. Gong Zhang et al. [13] have prepared sol gel derived CuO doped SnO$_2$ nanosized powder for gas sensor applications and obtained grain size in the order of 20nm. More et al. reported the incorporation of 9 wt% of Cu in SnO$_2$ by solvent evaporation method and investigated the nature of gas sensing bahaviour at various annealed temperatures [14]. Hu et al. studied the effect of Cu and Rh on optical properties of SnO$_2$ nanocrystallites and concluded that the dopant Cu leads to more effective localization of free electrons at the surface defects of the host material than Rh dopant [15].

Most studies reported in the literature have dealt mainly with gas sensitivity and conductivity of the tin dioxide doping systems and less care has been devoted to the microstructure and optical parameters [15]. In the present work we have synthesized pure and Cu doped SnO$_2$ nanopowders with two Cu doping concentration of 10 and 20 wt.% using chemical precipitation technique. The doping effect of Cu metal ions on the structure,

optical, electrical and electrochemical properties of SnO_2 nanocrystalline materials have been investigated.

2. Experimental procedure

The pure and Cu doped SnO_2 nanopowders were prepared by chemical precipitation method. In a typical experimental procedure, $SnCl_4.5H_2O$ (analytical grade) was dissolved in deionized water to make 0.1M solution. Then $NH_3.H_2O$ was added in to the solution drop wise under strong stirring until the pH of the solution reaches to 8. When the reaction completed, an azury precipitate was obtained. This precipitate was washed with deionized water more than 5 times to remove the Cl^- ions. Then the product was dried at 105°C for 5 hours. The final product was white colour powder. Cu doped SnO_2 were prepared in a similar manner, by adding 10 and 20 wt.% of $CuSO_4.5H_2O$ into $SnCl_4.5H_2O$ solution. In both cases, the products were light greenish in colour. Finally, both the pure and Cu doped SnO_2 powders were annealed at 600°C for 5 hours under ambient atmosphere.

2.1 Characterization

The prepared powders were carefully subjected to the following characterization studies. Powder XRD pattern was recorded on Bruker diffractometer within the 2θ range of 10 to 80° using CuKα as X-ray source (λ = 1.5406Å). Transmission Electron Microscopy (TEM), Selected-area Electron Diffraction (SAED) was recorded on a Technai G20-stwin High Resolution Electron Microscope (HRTEM) using an accelerating voltage of 200 kV. The optical properties were analyzed by UV-VIS diffusion reflectance spectroscopy using CARY 5E UV-VIS-NIR spectrophotometer in the wavelength range of 200 – 800 nm. All the samples were pressed into pellet form and contacts were made using silver paste as electrode and the temperature dependent resistance measurements were performed by four-probe electrode method. Cyclic voltammetric (CV) experiments were performed with a CHI 760 electrochemical analyzer, in single compartmental cells using tetrabutylammonium perchlorate as a supporting electrolyte. The electrochemical behavior of pure and Cu (20 wt. %) doped SnO_2 at a scan rate of 0.1 Vs^{-1} in the potential range +2.0 to -2.0 V were recorded. The following three-electrode configuration was used; a glassy carbon electrode as the working electrode, a Pt-wire as the auxiliary electrode, and an Ag/AgCl electrode as the reference electrode.

3. Results and discussion

3.1 XRD analysis

Fig.1 shows the XRD pattern of pure and Cu (10 and 20 wt.%) doped SnO_2 nanopowders annealed at 600°C for 5 hours. All the samples are identified as tetragonal rutile type SnO_2 phase and the results are in good agreement

with the standard JCPDS (41-1445) data. It can be noted that there are no peaks corresponding to Cu or CuO phase. This leads to the conclusion that doping of SnO_2 with Cu has occurred. There are two possible doping mechanisms of SnO_2 with Cu: substitutional and interstitial. In our case some Sn^{4+} ions are replaced with Cu^{2+} ion based on the comparable radii of Sn^{4+} and Cu^{2+} (0.57Å and 0.69Å, respectively) [16]. The oxygen-ion vacancies created by substitutional doping of Sn^{4+} with Cu^{2+} are charged compensated by electron holes, if the sample is annealed in air. The lattice parameters (a & c) and unit cell volume reduces upon doping of Cu (see table.1). These results are in good agreement with the literature values [16].
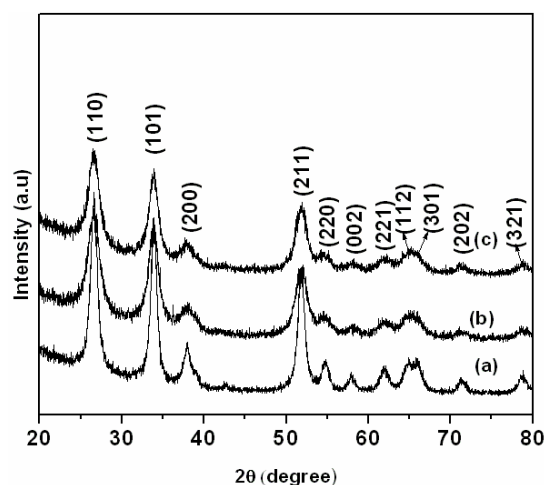
Fig. 1. XRD pattern of a) Pure and b) Cu 10 wt.% c) Cu 20 wt.% doped SnO_2. All the three samples have been annealed at 600°C for 5 hours in air.

The average grain size of the nanoparticles were calculated based on Scherrer's equation

$$d = \frac{K\lambda}{\beta\cos\theta}$$

where d is the mean crystalline size, K is the constant taken as 0.89, λ is the wavelength of the incident beam, β is the full width at half maximum

Table 1 Lattice parameters of pure and copper doped SnO_2.

Samples	a (Å)	c (Å)	Volume (Å³)
Pure SnO_2	4.727	3.186	71.189
SnO_2 + Cu 10 wt. %	4.725	3.185	71.107
SnO_2 + Cu 20 wt. %	4.723	3.185	71.046

The average crystalline size was found to be around 10 nm, 8 nm and 6.5 nm for pure and 10 & 20 wt.% Cu doped samples respectively. This decrease in grain size of SnO_2 suggests that the growth is suppressed due to doping of Cu into Sn-site [17]

3.2 TEM analyzes

Fig. 2 shows the TEM pictures of a) pure b) 10 wt.% Cu and c) 20 wt.% Cu doped SnO_2 nanopowders annealed at 600°C for 5 hours. Both pure and Cu doped samples consist of spherical shaped nanoparticles. The average particle size of pure SnO_2 is around 8-11 nm. For Cu 10 & 20 wt.% doped SnO_2, the particle size is between 7-9 nm and 5-7 nm respectively. These results are in good agreement with the XRD results. Ming You et al. [17] have reported the average particle size of SnO_2 – CuO nanocomposites to be 80 – 90 nm, which is higher than the values obtained in the present work. The SAED 'halo' ring patterns (Fig. 2d) confirm that both the pure and Cu doped nanopowders are polycrystalline in nature.
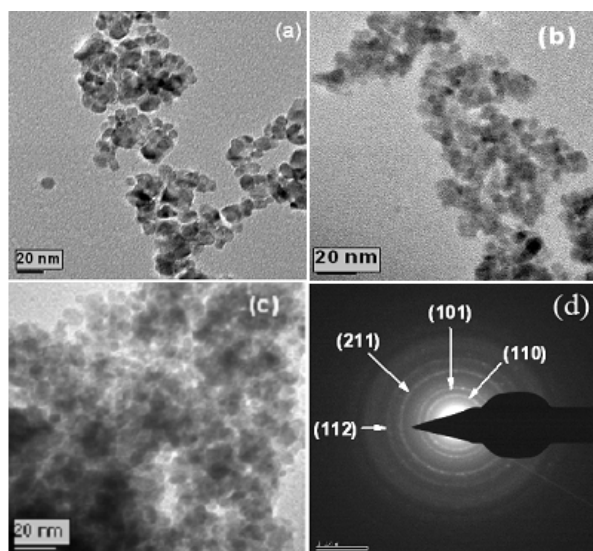
Fig. 2 TEM micrograph of SnO_2 powder a) Pure SnO_2 b) Cu 10 wt.% c) Cu 20 wt.% doped samples d) SAED pattern of pure and Cu-doped SnO_2.

3.3 UV-VIS Diffuse Reflectance Spectral analysis

Fig. 3 shows the UV-VIS diffuse reflectance spectra of pure and Cu doped SnO_2 nanopowders annealed at 600°C for 5 hours. The band gap energies calculated using Kubelka – Munk (K-M) model [18] is described below. The K-M model at any wavelength is given by

$$\frac{K}{S} = \frac{(1 - R_\infty)^2}{2R_\infty} \equiv F(R_\infty)$$

$F(R_\infty)$ is the so called remission or Kubelka – Munk function, where

$$R_\infty = R \text{ sample / } R \text{ standard}$$

where R is the percentage of reflectance [19]. A graph is plotted between $[F(R_\infty)h\upsilon]^2$ Vs $h\upsilon$ and the intercept value is the band gap energy [20] (see in fig.4).
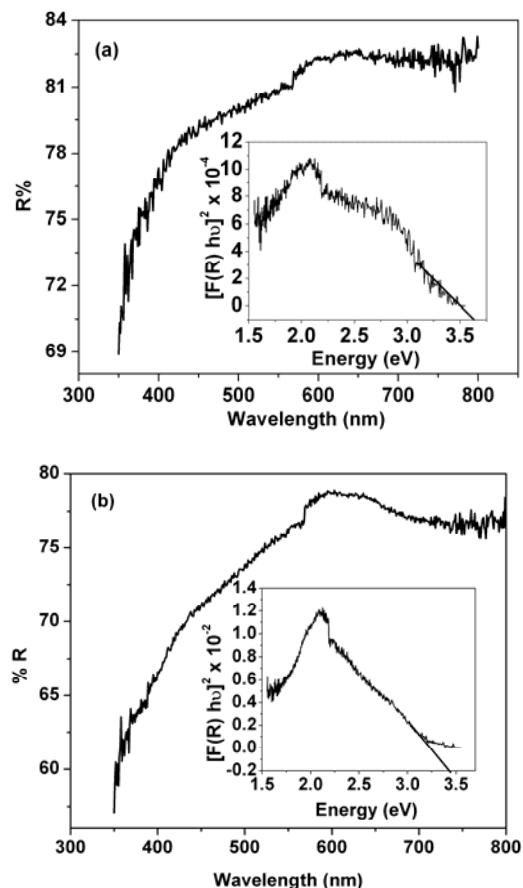
Fig. 3. UV-DRS spectrum of SnO_2 powder a) Pure SnO_2 b) Cu (20 wt.%) annealed at 600°C for 5 h.

It can be seen that the spectra of Cu-doped SnO_2 displayed a considerable red shift in the band gap transition with the increasing dopant content. The E_g value for pure SnO_2 is 3.56 eV, which is in good agreement with the reported values [21]. The Cu doped SnO_2 materials exhibit lower band gap energies of 3.31 eV and 3.28 eV for 10 and 20 wt.% respectively. Similar decrease in the band gap of SnO_2 has been reported for doping with other transition metals like Zn, Mg, Co, and In [22]. The observed decrease in band gap energy can be attributed to the charge-transfer transitions between the copper ion S electrons and the SnO_2 conduction or valence band. (S_2P exchange interaction)

3.4 Resistance measurement

Fig. 4 shows resistance – temperature profile of pure and Cu 20 wt.% doped SnO_2 nanopowders annealed at 600°C. The synthesized nanopowders were pressed in the form of pellet and electrode contact was made using silver paste.
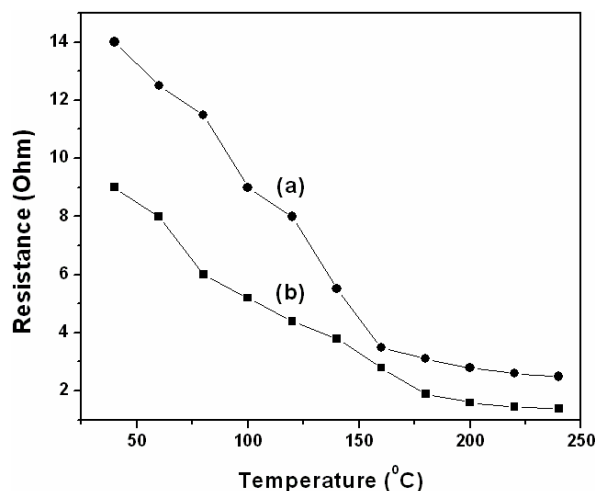
Fig. 4 The variation of resistance with temperature for
a) pure b) Cu (20 wt.%) doped SnO_2 Nanopowders.

The decrease in resistance with increase in temperature (above 50°C) could be attributed to negative temperature coefficient and semiconducting nature of the pure and Cu doped SnO_2 nano powders.

The Cu doped sample shows lower resistance than the pure SnO_2 material. This is due to the donation of free electrons by the Cu ions. The resistivity of pure and Cu 20 wt. % doped SnO_2 at ambient temperature was found to be 13.18 Ω cm and 8.48 Ω cm which implies the enhancement in electrical conductivity of Cu doped SnO_2. The result confirms that both pure and Cu doped SnO_2 materials were having good electrical response with temperature. These types of materials are preferable of gas sensing applications.

3.5 Cyclic voltammetric (CV) measurement

Fig. 5 shows the cyclic voltammogram studies of pure and Cu doped (20 wt.%) SnO_2 nanopowders. The electrochemical parameters such as cathodic peak potential (E_{pc}) and anodic peak potential (E_{pa}) were measured. Both the pure and Cu (20 wt.%) doped SnO_2 samples show irreversible oxidation only (cathodic peak 1.42 V) and reversible reduction anodic peak (-0.5 V) and cathodic (-0.9 V) peak.
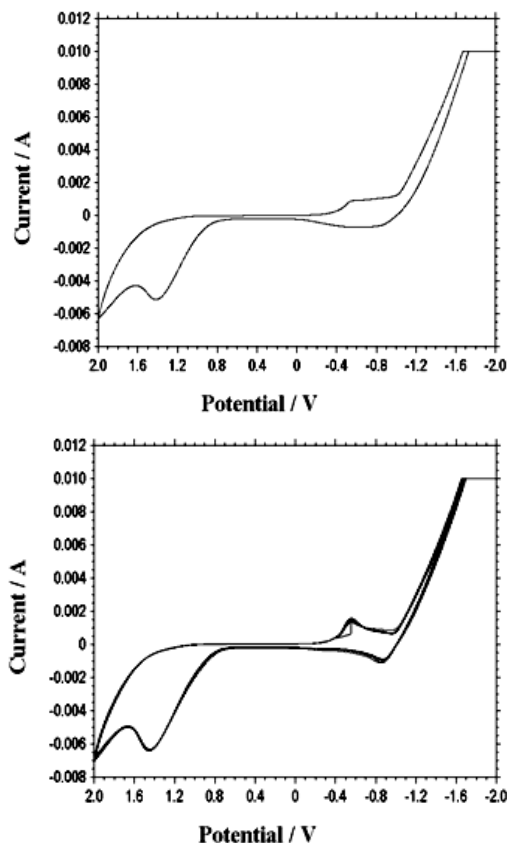
Fig. 5. Cyclic voltammogram of SnO₂ nanopowder
a) pure b) Cu (20 wt.%) doped SnO₂ nanopowders

The reduction peaks are found to be quasi-reversible in nature with peak - to- peak separation value (ΔE_p is 400 mV). Based on this result, it can be concluded that both the samples possesses electrochemical behavior. The cyclic voltammogram shows that the peak positions of pure and Cu doped sample is the same, but the Cu doped sample the peak intensity is increased. This implies that the reduced metallic Cu enhances the good electrochemical behavior when compared to that of pure SnO_2.

4. Conclusions

The pure and Cu doped SnO_2 nanopowders were prepared by chemical precipitation method. The average crystalline size of pure SnO_2 was found to be around 10 nm. The crystal structure of the SnO_2 does not change with the introduction of Cu, but the crystalline size decreases to 8 nm and 6.5 nm for Cu (10 & 20 wt.%) respectively. These results are in good agreement with the TEM results. The cyclic voltammetric studied confirmed that Cu doped sample have good electrochemical behavior when compare to pure SnO_2 sample. The UV- VIS diffusion reflectance spectroscopy (DRS) and temperature dependent resistance results confirm the Cu doping have positive influence on the optical and electrical properties of tin dioxide nanocrystalline material.

References

[1] S. S. Pan, C. Ye, X. M. Teng, G. H. Li, J. Phys. D: Appl. Phys. **40,** 4771 (2007)

[2] H. Zhu, D. Yang, G.Yu, H. Zhang, K. Yao, Nanotechnology. **17,** 2386 (2006)

[3] F. Du, Z. Guo, G. Li, Mater. Lett. **59,** 2563 (2005)

[4] J. Duan, S. Yang, H.Liu J.Gong, H. Huang, X. Zhao, R. Zhang, Y. J. Du, Am. Chem. Soc. **127,** 6180 (2005)

[5] Y. Liu, E. Koep, M. Liu, Chem. Mater. **17,** 3997 (2005)

[6] Z .R Dai, J.L Gole, J.D Stout, Z. Wang, J. Phys. Chem. B **106,** 1274 (2002)

[7] J. Q. Hu, X. L Ma, N. G Shang, Z. Y. Xie, N. B. Wong, C. S. Lee, S. T. Lee, J. Phys. Chem. B **106,** 3823 (2002).

[8] F. Pourfayaz, A. Khodadadi, Y. Mortazavi, S. S. Mohajerzadeh, Sens. Actuators B **108,** 172 (2005).

[9] A. Majid, J. Tunney, S. Argue, D. Kingston, M. Post, J. Margeson, J. Graeme, J. Sol-Gel Sci. Technol. DOI 10.1007/s10971-009-2108-x.

[10] L. M. Fang, X. T. Zu, Z. J. Li, S. Zhu, C. M. Liu, L. M. Wang, F. Gao, J. Mater. Sci. Mater. Electron. **19,** 868 (2008).

[11] H. Y. Jin, Y. H. Xu, G. S. Pang, W. J. Dong, Mater. Chem. Phys. **85**, 58 (2004).

[12] C.T. Lee, F.S. Chen, C.H. Lu, J. Alloys Compd. **490,** 407 (2009).

[13] G. Zhang, M. Liu, Sens. Actuators B **69**, 144 (2000).

[14] P. S. More, Y. B. Khollama, S. B. Deshpande, S. K. Date, R. N. Karekar, R. C. Aiyer, Mater. Lett. **58**, 205 (2003).

[15] C. X. Hu, Y. S. Wu, H. Y. Wei, Y. C. Shi, L. L. Wu, J. Mater. Sci. **40**, 6301 (2005).

[16] Vivek Kumar, Shashwati Sen, K.P. Muthe, N. K. Gaur, S. K. Gupta, J. V. Yakhmi, Sens. Actuators B: Chemical **138,** 587 (2009).

[17] M. A. Ming-you, H. E. Ze-qiang, X. Z. Bing, H. Ke-long, X. Li-zhi, W. Xiang-ming, Trans. Nonferrous Met. Soc China. **16,** 791 (2006).

[18] H. Zhu, D. Yang, G. Yu, H. Zhang K. Yao, Nanotechnology. **17**, 2386 (2006).

[19] G. Kortum, Reflectance Spectroscopy (Springer-Verlag, Newyork, 1969).

[20] S. Mosadegh Sedghi, Y. Mortazavi A. Khodadadi, Sen. Actuators B: Chemical. **145,** 7 (2010).

[21] C. M. Liu, X. T. Zu, Q. M. Wei, L. M. Wang, J. Phys D: Appl. Phys. **39,** 2494 (2006).

[22] C. Drake, S. Seal, Appl. Phys. Lett **90,** 233117 (2007).

---

[*]Corresponding author: sekar2025@gmail.com